



Effects of acid accelerators on hydrogen generation from solid sodium borohydride using small scale devices

Sankaran Murugesan, Vaidyanathan (Ravi) Subramanian*

Department of Chemical and Metallurgical Engineering, University of Nevada,
Reno, NV 89557, USA

ARTICLE INFO

Article history:

Received 15 August 2008

Received in revised form 15 October 2008

Accepted 16 October 2008

Available online 1 November 2008

Keywords:

Hydrogen generation

Small scale device

Borohydride

Acid accelerator

ABSTRACT

This work describes hydrogen generation using a heterogeneous chemical system for small scale portable applications. Hydrogen generation using acidified water and solid sodium borohydride (NaBH_4) is presented. The effects of two modes of contacts – (1) a flow through type and (2) a diffusion type – contact in a 5 mm^3 device are discussed. The effects of contacting several mineral and benign acids with NaBH_4 are compared by monitoring hydrogen yield. Among the mineral acids examined, HCl generates a maximum hydrogen yield of 97% of the theoretical yield at 3N concentration. The benign acids are required in higher concentration compared to mineral acids. Formic acid produces 87% of the hydrogen yield at 12N. The products of the reaction have been characterized using scanning electron microscopy and X-ray diffraction. A combination of acid strength, porosity of the interface, and solubility of the byproducts contributes to the different hydrogen yields in the presence of various acids.

Published by Elsevier B.V.

1. Introduction

Fuel cells have attracted immense interest as energy sources for portable devices [1]. Hydrogen produced by chemical conversion of an energy source, can be used by the fuel cells to generate electricity to power portable devices. Of specific interest to this work are consumer electronics [2] and devices for defence applications such as covert reconnaissance operations where miniaturization of these hydrogen generators are essential [3]. Currently, the hydrogen generators that power miniature devices typically occupy a significant fraction of the total device volume. This is a limitation since large power sources not only make the device bulky, but also compromise with the application of the systems (such as arthropods used in reconnaissance missions). The challenges lie in miniaturization of the energy source to a fraction of the device size [4,5]. Another limiting factor in employing fuel cell in portable devices, is the selection of appropriate hydrogen source that can produce hydrogen with a high efficiency [6,7]. An ideal energy source is one that has minimal weight and volume, occupies a small fraction of the device volume, and still produces enough hydrogen efficiently from the standpoint of long-term operations.

The light elements of I, II and III group (Li, Na, Mg, B, and Al) form a variety of metal hydrogen complexes [8]. The hydrides of boron (tetrahydrides) have been of primary interest as they react with water to generate high purity hydrogen in fuel cells [9,10]. Among tetrahydrides, sodium borohydride is an attractive solid source of hydrogen due to its high gravimetric energy density (9300 Wh kg^{-1}) [11]. Sodium borohydride reacts with water and generates hydrogen gas of high purity [12,13]. However, this reaction is sluggish due to pH shift by stabilized borate ion. Since the rates of hydrolysis are slow, metal catalysts are often used to improve kinetics [14]. Recently, metal borides such as CoB and NiB have been used as catalyst for hydrogen generation and demonstrate high rates of hydrogen release with better kinetics compared to pure metal catalyst [15–19]. The above studies have been performed with sodium borohydride (NaBH_4) stabilized in alkaline solution (1–10% NaOH or KOH) using generators that are large (several centimeters in dimensions).

Small scale devices have space constraints. Alkali stabilized NaBH_4 systems typically require the use of Co-Catalysts for efficient hydrogen production [20–22]. If one considers using catalysts in microdevices, aspects such as catalyst activity, additional complexity associated with loading and uniform distribution of the catalyst, and loss of volume associated with the catalyst has to be considered. Alternately, the use of solid NaBH_4 powder instead of alkali stabilized borohydride can allow implementing simpler methods to load the hydrogen generator made of silicon, which is the standard material for miniature device fabrication [23,24].

* Corresponding author at: Chemical and Metallurgical Engineering Department, Room 310, LMR 474, Mail stop 388, University of Nevada, Reno, NV 89557, USA.
Tel.: +1 775 784 4686; fax: +1 775 327 5059.

E-mail address: ravisv@unr.edu (V. Subramanian).

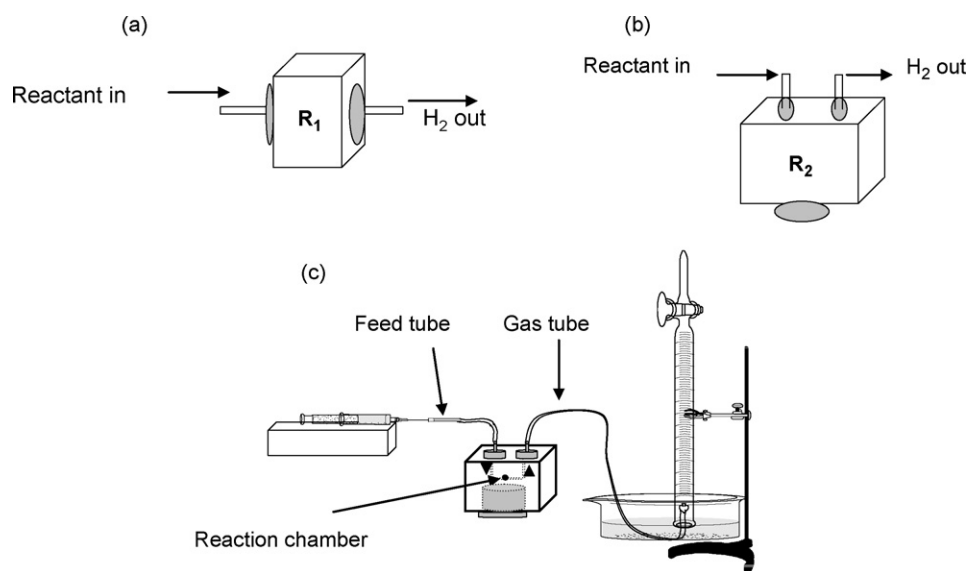


Fig. 1. The schematic diagram of the small scale hydrogen generator: (a) flow through type (R_1), (b) diffuse through type (R_2), and (c) the experimental setup and cross-sectional view of R_2 . (Dimensions of the generators R_1 and R_2 are provided in Table 1.)

Hitherto production of hydrogen by contacting liquid with a solid source of hydrogen in miniaturized device and the effects of hydrogen generator design on hydrogen yield is not yet examined. In this paper we examine the hydrogen yield from NaBH_4 powder using two custom built small scale devices of 5 mm^3 volume. The effect of catalyst-free production of hydrogen using various acids as accelerators of hydrolysis rates has been examined. The reaction products formed in the presence of different acid accelerators and their effects on the hydrogen generation has been examined using scanning electron microscope and X-ray diffraction.

2. Experimental details

2.1. Materials

The mineral acids HCl , H_2SO_4 , HNO_3 , H_3PO_4 and carboxylic acids, HCOOH and CH_3COOH were purchased from BDH-Aristar (VWR, 36.5–38% assay). Sodium borohydride powder was obtained from Sigma–Aldrich (Rohm and Hass, reagent grade $\geq 98.5\%$). DI water ($1.2 \text{ M}\Omega$ resistance), obtained from an in-house Millipore® water purification system, and was used to prepare stock solution of acids at different concentrations. Experiments involving water alone were also performed with Millipore DI water. X-ray diffraction (XRD) was performed using a Philips APD 1740 system equipped with a graphite crystal monochromator and $\text{Cu K}\alpha$ radiation ($\lambda = 1.54 \text{ \AA}$) between the 2θ range of $20\text{--}80^\circ$. XRD was carried out using specially prepared polished quartz

cut 6° from (0001) crystal plane with a cavity of dimension of 3 mm diameter and 1 mm depth (Gem Dugout X-ray Diffraction Products). A field emission-scanning electron microscope (FESEM, Hitachi, S-4700) was used to analyze the morphology of the reaction products. Due to the hygroscopic nature of NaBH_4 , all the parts of the reactor were completely dried prior to starting an experiment and the NaBH_4 was loaded into the generators in a glove box. Stoichiometric amount of liquids were added to obtain hydrogen.

2.2. Generator design and calculations

2.2.1. Flow through type generator (R_1)

The two hydrogen generators were designed with a volume of 5 mm^3 and fabricated with Teflon® as the base material. In the first generator (R_1), threaded hollow connectors containing two tubes (feed and gas tubes) made of Teflon® are snugly fit on the inside of the housing on either sides on the Teflon® block as shown in Fig. 1a. Both flow screws are threaded to the Teflon® base through an O-ring to prevent the leakage of water at the feed end and at the gas end towards the exit. The detailed dimensions of the generators are provided in Table 1 and an exploded view of the generator assembly is provided in supplementary figure S1. A porous ceramic frit is placed at the gas outlet side of the hollow connector, to allow only the gas to diffuse out of the reaction chamber. This also helps in retaining the liquid reactant and assist in the complete utilization of liquid for hydrolysis of sodium borohydride.

Table 1
Dimensions of the flow through type (R_1) and the diffusion type (R_2) hydrogen generators.

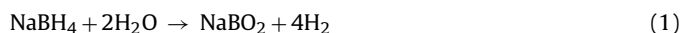
Specifications	Dimensions of the hydrogen generators	
	R_1	R_2
Teflon block housing (length \times width \times height)	15 mm \times 15 mm \times 12 mm	25 mm \times 25 mm \times 15 mm
Threaded hole (diameter, length)	6 mm, 5 mm	11 mm
Threaded depth in the reactor	5 mm	7 mm
Reaction chamber (depth, width)	1.6 mm, 2 mm	1.6 mm, 2 mm
Volume of the reaction chamber	5 mm^3	5 mm^3
Diameter of reactant inlet and gas outlet tubes	1 mm	1 mm
	Frit before gas outlet thread (diameter, thickness = 3.5, 1.6 mm)	Distance between micro-channel = 3 mm
	Feed tube diameter = 2 mm, gas tube diameter = 2 mm	

2.2.2. Diffusion through type generator (R_2)

In the second generator (R_2), the liquid reactant is contacted with the NaBH_4 by the downward movement while the generated hydrogen flows upwards through a nearby exit. Unlike R_1 , this design does not require a frit to prevent the movement of solid reactants. A 50 μl Hamilton[®] syringe mounted over a syringe pump was used to deliver controlled quantities of liquid into the generators using the feed tube. The flow of liquid in R_2 is also facilitated by the capillary action of a fine channel from the reactor inlet to the reaction chamber as shown in Fig. 1b. Therefore pressure drop is expected to be lower in R_2 than in R_1 . As the gas flows upward, movement of solid particles from the reaction chamber can be avoided. The hydrogen evolved is collected by the gas displacement method as shown in Fig. 1c.

2.2.3. Calculations

The theoretical hydrogen yield from NaBH_4 is calculated on the basis of the following reaction:



One mole of NaBH_4 reacts with two moles of water producing four moles of hydrogen. This translates to 905 mm^3 of hydrogen per mm^3 of reactants at NTP conditions. The reactants include stoichiometric amounts of water and NaBH_4 . The volume of acidified water is assumed to be negligibly different from plain water and hence all calculations are reported with respect to water. The percent hydrogen yield is calculated based on the ratio of actual hydrogen obtained (mm^3) to the theoretical hydrogen (905 mm^3) at NTP conditions.

The flow rate of liquid reactants was fixed at $1 \mu\text{l min}^{-1}$. Such low flow rates mimic the contacting processes in miniaturized devices [25,26]. The low flowrate allows enough time for intimate mixing between the reactants and ensures complete utilization of the liquid reactant without inundating the pathways for hydrogen transport. Further, the miniature devices used in defense applications, such as cognitive anthropods, requires very low power. Their power needs can be met by just a few tens of milliliters of hydrogen. To operate such devices, a slow and steady release of hydrogen is desired. These requirements were at the basis of choosing a low flowrate for the liquid addition. Scale up of hydrogen production can be achieved by adding several of these devices in parallel.

3. Results and discussion

3.1. Effects of mode of contact on hydrogen yield

Fig. 2 shows the effects of the generator design on the hydrogen yield with the addition of water. There is a lag time of approximately 10 s between the beginning of water addition and the point when the first bubble of hydrogen is noticed in the water column. The hydrogen yield with stoichiometric amounts of water addition was noted to be 26% and 35% with the generators R_1 and R_2 , respectively. The low yields are attributed to the partial conversion of the NaBH_4 . The improvement in the hydrogen yield with R_2 is attributed to the mode of contact between the water and the solid borohydride.

3.2. Importance of acid accelerators

The reaction of NaBH_4 with water results in a low hydrogen yield due to pH stabilization of the reaction medium. This pH stabilization is caused by the formation of the strongly basic metaborate ions [27]. The addition of acids delays the formation of the metaborate ions by shifting the pH of the reaction medium to lower values which allows improved hydrogen yield. Thus, for a simple and rapid

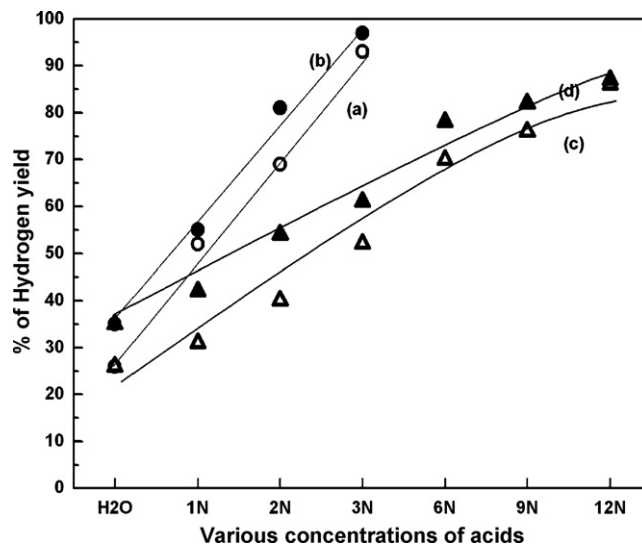


Fig. 2. Comparison of the hydrogen yield obtained after the reaction of NaBH_4 with different concentrations of HCl in the generators (a) R_1 , (b) R_2 and HCOOH in (c) R_1 , (d) R_2 . The flowrate of the liquid was maintained at $1 \mu\text{l min}^{-1}$.

generation of hydrogen, without the use of catalyst, one can consider acid accelerators. The choices that are available for increasing the hydrogen yield with acids, include selecting the type of acid and/or changing the acid concentration. The effects of both these choices on the hydrogen yield from NaBH_4 are reported below.

Two different types of acids were used: mineral acids with interfering anions and benign acids with non-interfering ions. Bench scale studies have shown that stronger acids can lead to greater hydrogen generation rates by reaction of acids with sodium metaborate to form tetraborate [28,29].

Fig. 2 shows the effects of the water acidified with HCl and HCOOH. The addition of acidified water is noted to improve the hydrogen yield compared to the addition of water. For example, the addition of 1N HCl improves the hydrogen yield from 26% to 52% in the generator R_1 . It can also be noted that as the concentration of the HCl increases the hydrogen yield from the NaBH_4 increases (Fig. 2a). The hydrogen yield improves from 52% to 93% when the HCl concentration increases from 1N to 3N. When one switches from the generator R_1 to R_2 , the hydrogen yield is observed to be 97% with the addition of 3N HCl (Fig. 2b). Similar improvements in the hydrogen yield were noted with the addition of 1N solution of HCOOH. An almost linear increase in the hydrogen yield from 31% to 70% is noted when HCOOH concentration changes from 1 to 6N as shown in Fig. 2c. At concentrations greater than 6N, the hydrogen yield was noted to be 86% at 12N. The hydrogen yield with generator R_2 is 87% with 12N HCOOH.

The percentage of hydrogen yield obtained from the reaction of NaBH_4 with water and various concentrations of other mineral and benign acids are compared in Table 2. Several observations can be drawn from a comparative study of these results. For instance, it is evident that all the mineral acids facilitate an increase in the hydrogen yield with an increase in acid concentration. The hydrogen yields are significantly lower with the addition of HNO_3 and H_3PO_4 as shown in Table 2 compared to HCl and H_2SO_4 . Benign acids in general are required in higher concentrations (9–12N) to provide a hydrogen yield similar to the mineral acids such as HCl and H_2SO_4 . Acetic acid shows a maximum of 78% hydrogen yield at a concentration of 9N. Further, a comparison of the performance of the generators show that the flow-through type generator R_1 generally results in a lower hydrogen yield compared to the diffuse-through type generator R_2 at most acid concentrations. Three acids are iden-

Table 2Hydrogen yield from the hydrolysis of NaBH_4 in the presence of various acids of different concentrations.

Different acids	Percentage ^a of hydrogen yield from NaBH_4													
	H ₂ O		HCl		H ₂ SO ₄		HNO ₃		H ₃ PO ₄		HCOOH		CH ₃ COOH	
	Reactors													
	R ₁	R ₂	R ₁	R ₂	R ₁	R ₂	R ₁	R ₂	R ₁	R ₂	R ₁	R ₂	R ₁	R ₂
Conc.	26	35												
1N			52	52	34	60	33	35	26	33	31	42	29	36
2N			69	81	69	78	55	63	39	41	40	44	43	44
3N			93	97	83	96	46	50	41	52	52	57	57	62
6N											76	68	80	67
9N											77	82	86	78
12N											86	87	76	51

^a Percentage of hydrogen yield is calculated by using the theoretical hydrogen yield of NaBH_4 (905 mm^3).

tified that demonstrates very high hydrogen yield. This includes 3N HCl (yield 97% in R₂), 3N H₂SO₄ (96% in R₂), and 12N HCOOH (87% in R₂). The results presented in Fig. 2 and Table 2 shows that hydrogen production using a solid–liquid heterogeneous chemical system can be efficiently performed using small scale generators by employing acid accelerators without the use of any catalysts.

3.3. Effects of acid addition on the initial rates of hydrogen generation

The rate of hydrogen evolution for mineral acids at 3N can be estimated from the yield vs. time data. A plot of hydrogen evolved in terms of mm^3 hydrogen per mm^3 of reactants (the reactant includes both the volume of acidified water and volume of NaBH_4) with respect to time is given in Fig. 3 for R₁ and Fig. 4 for R₂. The dotted line represents the theoretical limit in the hydrogen production using a unit volume of reactants. From these results, one can infer that the addition of HCl gives a better overall hydrogen yield than H₂SO₄. However, depending upon the generator, during the first 10–30 min of the reaction, the addition of H₂SO₄ results in a higher rate of hydrogen generation compared to HCl of similar concentration. Since the generator R₂ provides a better hydrogen rate as well as yield than R₁ with acidified water, the rates are examined for R₂. The initial rate of hydrogen release is calculated by considering the

hydrogen yield during the first 10 min of the reaction using the data in Fig. 4. This analysis shows that, H₂SO₄ gives the maximum hydrogen release rate of $83 \text{ mm}^3 \text{ min}^{-1}$ followed by HCl ($57 \text{ mm}^3 \text{ min}^{-1}$). It is also noteworthy to mention here that due to the high rates of hydrogen generation, R₂ facilitates the liberation of ~70% of the total generated hydrogen (600 mm^3) in roughly half the time used by the generator R₁. The results of Figs. 3 and 4 confirm the better mode of contact established between the heterogeneous reactants through the design of the generator R₂.

3.4. Factors that influence hydrogen yield in heterogeneous systems

From the preceding sections it can be inferred that the hydrogen yields vary with the type of acids used in both the generators. This can be attributed to multiple reasons. Firstly, the strength of the acid can be expected to play a crucial role on the hydrogen yield. Secondly, the fact that this chemical system is heterogeneous (liquid–solid); it raises the question about the role of interface in the hydrogen yield. Thirdly, it is not unreasonable to expect that boron chemistry can contribute to the changes noticed in the hydrogen yield. These possibilities have been examined and are the subjects of discussion in the remaining part of this paper.

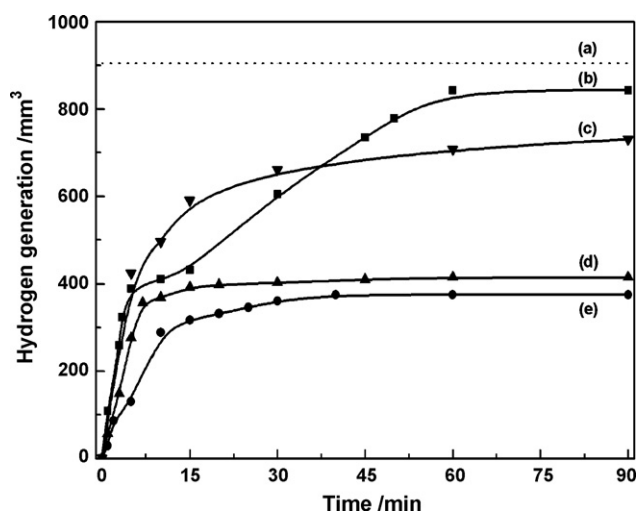


Fig. 3. The change in the hydrogen yield with time during the reaction of NaBH_4 with acidified water using reactor R₁ is shown. Curve (a) represents the theoretical amount of hydrogen that can be generated on reaction of NaBH_4 with water. The hydrogen yield after the addition of a 3N solution of (b) HCl, (c) H₂SO₄, (d) H₃PO₄, and (e) HNO₃ at a flowrate of $1 \mu\text{l min}^{-1}$ is shown. All volumes are expressed on the basis of 1 mm^3 of reactants.

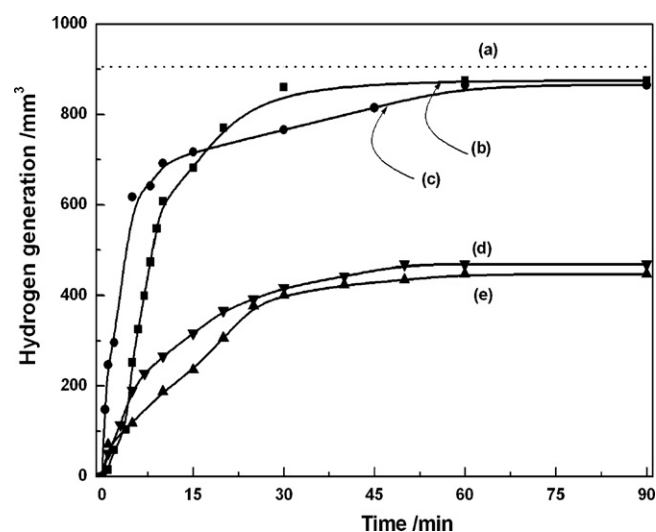


Fig. 4. The change in the hydrogen yield with time during the reaction of NaBH_4 with acidified water using reactor R₂ is shown. Curve (a) represents the theoretical amount of hydrogen that can be generated on reaction of NaBH_4 with water. The hydrogen yield after the addition of a 3N solution of (b) HCl, (c) H₂SO₄, (d) H₃PO₄, and (e) HNO₃ at a flowrate of $1 \mu\text{l min}^{-1}$ of the acidified solution. All volumes are expressed on the basis of 1 mm^3 of reactants.

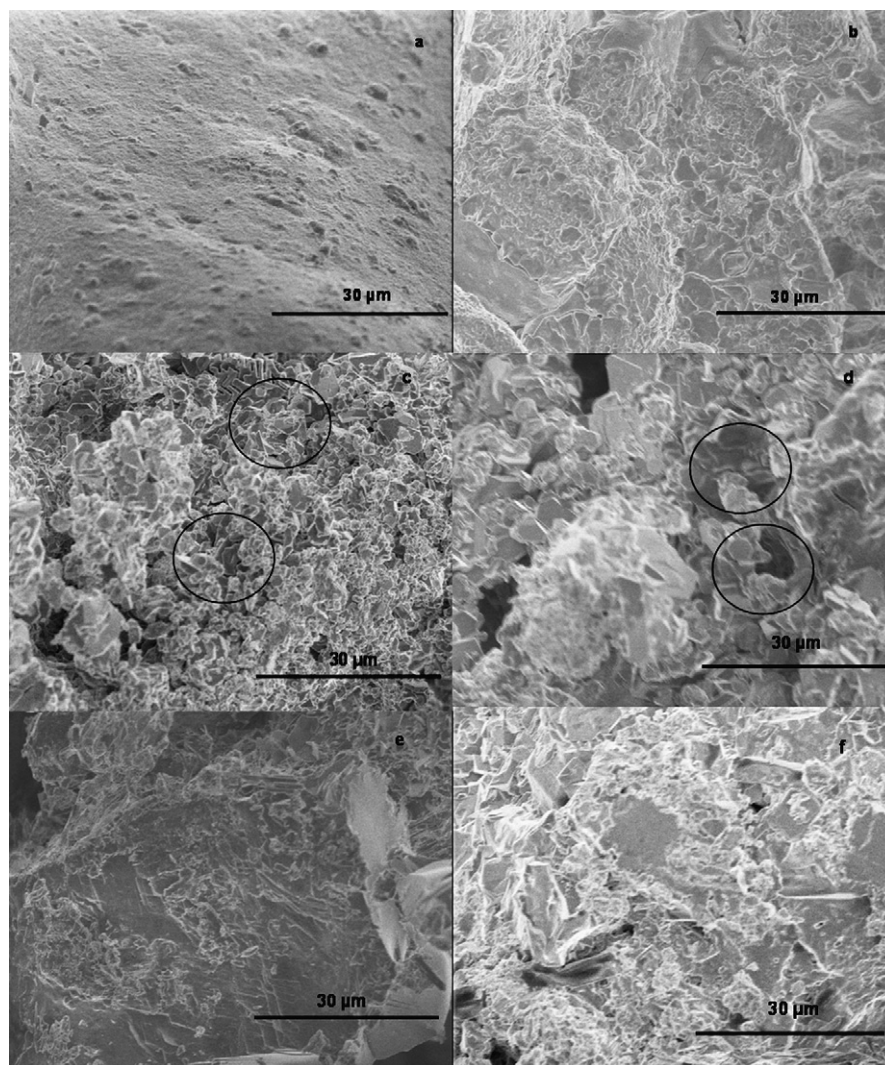


Fig. 5. SEM images of pure NaBH_4 powder (a) prior to reaction, after the reaction with (b) water, (c) 3N HCl, (d) 3N H_2SO_4 , (e) 3N HCOOH, and (f) 3N CH_3COOH . The liquid flowrates were maintained at $1 \mu\text{l min}^{-1}$ in all experiments.

3.4.1. Effects of acid strength

The strength of the acid is a measure of the dissociation of the acid in an aqueous media. The dissociation constant (estimated from pK_a values) are specific to the acids. In general, strong acids have a high dissociation constant (low pK_a values) compared to weak acids. The acids considered in this study have a wide ranging pK_a values: HCl (−8), H_2SO_4 (−3), HNO_3 (−1.3), H_3PO_4 (2.12), HCOOH (3.77), CH_3COOH (4.76) [30,31]. Strong acids have a high dissociation constant and therefore release a large concentration of H^+ ions. The high concentration of H^+ ions promotes accelerated hydrolysis of the borohydride. The hydrogen yield can be enhanced by the release of H^+ ions as it drives the pH low [32]. Thus, the high hydrogen generation rate as well as the yield observed in the presence of HCl and H_2SO_4 compared to the other acids can be attributed to the low pK_a values of these acids.

3.4.2. Reaction interface and effects of interfering anions

The second possibility pertains to the heterogeneous nature of the chemical system. In heterogeneous systems, the reaction interface plays a crucial role in controlling the reaction rate and the hydrogen yield. The factors that can contribute to the role of interface include interface porosity and composition of the byproducts. In order to maximize hydrogen yield, the reaction interface should

permit the transport of the liquid reactant for further reaction with the unreacted NaBH_4 . Ideally, the interface should act as a wicking agent so that the contacting liquid reactant will be automatically and evenly distributed. Besides, the interface should demonstrate the necessary properties (such as porosity) to allow free movement of the reactants and the product (mainly hydrogen) out of the reaction zone. This can be facilitated by the formation of porous interface and/or byproducts that are highly soluble and hence can promote liquid transport. One can follow these changes at the interface using SEM and XRD. These techniques were used to examine the interface structure and its composition after the reaction to elucidate possible relationships between interface morphology and hydrogen yield.

SEM images of byproducts formed after the reaction with water, 3N HCl, H_2SO_4 , and HCOOH are shown in Fig. 5. The unreacted NaBH_4 has a porous surface due to the fine granular nature of the particles (Fig. 5a). Shortly after reaction with water the interface appears as a complete continuous layer with negligible porosity (Fig. 5b). On the other hand, it can be seen that the interface morphology has been significantly modified by the reaction with acidified water. A change in the roughness due to the formation of several pores along with the formation of cracks can be noted (circled locations in the images). In Fig. 5c, the SEM image of the

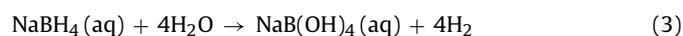
interface formed after reaction with HCl leads to denser and more uniform pores, whereas the pores are sparsely located on reaction with H_2SO_4 (Fig. 5d). It is important to mention that reaction with HCl and H_2SO_4 leads to the formation of these pores almost instantaneously. On the other hand, the reaction with HNO_3 and H_3PO_4 does not show the pore formation as explicitly noticed with HCl or H_2SO_4 .

In the case of the benign acids, no pore formation can be noticed with either formic acid or acetic acid. The surface appears to be unaffected after the addition of the benign acids (Fig. 5e and f). These observations imply that the weak acids at low concentrations do not facilitate the formation of a porous interface.

Instantaneous reaction with NaBH_4 is expected in the presence of highly dissociating strong acids such as HCl and H_2SO_4 . This causes a sudden generation of large volumes of hydrogen within the liquid–solid interface. The limited volume available in the generator interface forces this hydrogen to physically carve out a pathway downstream. This can be at the basis of the distinct pores noted at the interface on reaction with HCl and H_2SO_4 . Note that absence of such pore formation with the other acid such as HNO_3 , H_3PO_4 or the benign acids can be attributed to the lower hydrogen generation rates and yield following the reaction with these acids. The data from Table 2 shows that this can be offset by increasing the normality of the benign acid (12N HCOOH provides higher hydrogen yield than 3N HCOOH).

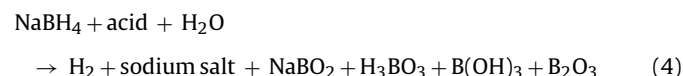
Another interesting observation can be made by comparing the hydrogen yield using benign acids with HNO_3 and H_3PO_4 . In spite of the low dissociation constant values of the benign acids, compared to mineral acid, the benign acids show higher hydrogen yields than H_3PO_4 and HNO_3 (Table 2). This means that the dissociation is not the only factor that influences hydrogen yield. It then raises the question: what causes the benign acids with lower dissociation constant to produce higher hydrogen yield than HNO_3 or H_3PO_4 ? One possible explanation could be that the solubility of the byproducts can be influencing the hydrogen yield. To verify this, a closer look at the byproducts formed after the hydrolysis of the NaBH_4 was pursued.

XRD was used to identify the composition of the interface products formed after the reaction with 3N acids. X-ray diffractograms obtained for NaBH_4 and the reaction products with water are given in Fig. 6. The peaks were identified with MDI Jade 6.5 database. The diffraction peaks in Fig. 6a corresponds to NaBH_4 (JCPDS card # 09-0386). The reaction of NaBH_4 with water yields different products (Eqs. (1)–(3)).



Eqs. (1)–(3) show that the products of reaction with water vary. NaBO_2 is the only peak detected among the byproducts following the reaction with water (JCPDS card # 37-0115, $2\theta = 29.06^\circ$) as shown in Fig. 6b. Peaks corresponding to NaOH and $\text{NaB}(\text{OH})_4$ could not be detected. From these observations, it can be inferred that the likely pathway for the hydrolysis of NaBH_4 in the presence of water is through Eq. (1).

When the different acidified water reacts with NaBH_4 , the likely products are corresponding sodium salts of the conjugate bases (anionic sodium salts) and boron compounds. A generalized form of reaction between NaBH_4 with any acid can be written as



where acid = HCl, H_2SO_4 , HNO_3 , H_3PO_4 , HCOOH and CH_3COOH .

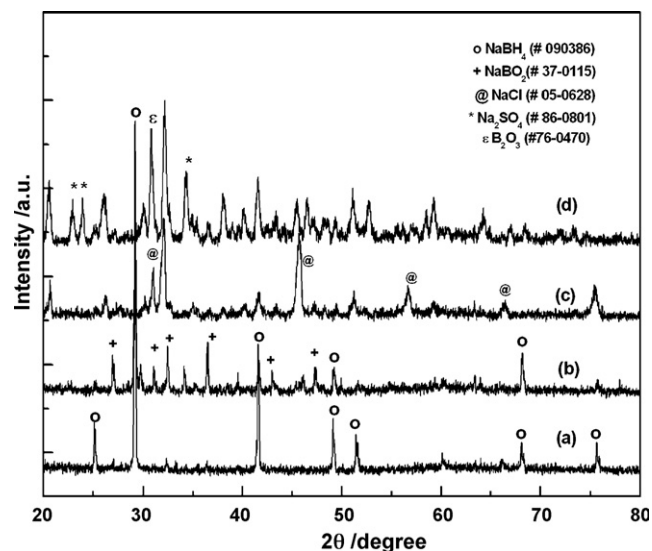


Fig. 6. XRD patterns of pure NaBH_4 powder (a) prior to reaction, after the reaction with (b) water, (c) 3N HCl, (d) 3N H_2SO_4 . The liquid flowrates were maintained at $1 \mu\text{l min}^{-1}$ in all experiments.

The XRD of NaBH_4 was compared to the XRD of the products formed with 3N HCl. In Fig. 6c, a peak corresponding to NaCl (JCPDS card # 05-0628) is evident as marked. Besides, another peak at $2\theta = 29.15^\circ$ is also distinctly noted. This could correspond to H_3BO_3 (JCPDS card # 23-1034). However, this peak is very close to the peak noted for NaBO_2 (JCPDS card # 37-0115, $2\theta = 29.06^\circ$). Hence, this peak could not be clearly identified. However, the fact that NaCl is detected from other peaks ($2\theta = 45.7^\circ$ and 56.9°), suggests that hydrogen is indeed produced through the route proposed in Reaction (4). Fig. 6d shows the XRD of the products formed after reaction with H_2SO_4 . The peaks $2\theta = 22.86^\circ$ and 32.98° corresponds to Na_2SO_4 (JCPDS card # 86-0801). In addition to these peaks, boron compounds such as B_2O_3 was identified from this reaction (JCPDS card # 76-0470, $2\theta = 31.22^\circ$).

The reaction of NaBH_4 with HNO_3 and H_3PO_4 (Fig. 7a–c) results in the formation of the corresponding anionic salts NaNO_3 (JCPDS

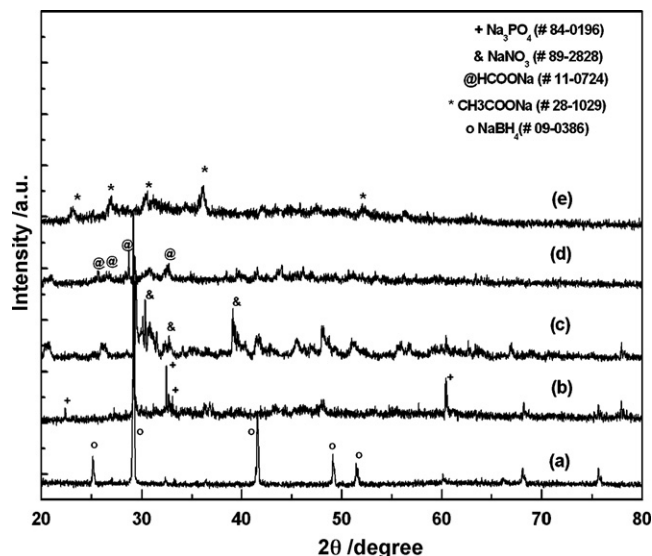


Fig. 7. XRD patterns of pure NaBH_4 powder (a) prior to reaction, after the reaction with (b) H_3PO_4 , (c) 3N HNO_3 , (d) 3N HCOOH , and (e) 3N CH_3COOH . The liquid flowrates were maintained at $1 \mu\text{l min}^{-1}$ in all experiments.

card # 89-2828, $2\theta = 29.45^\circ$) and Na_3PO_4 (JCPDS card # 84-0196, $2\theta = 33.72^\circ$). Along with these salts, a boron compound H_3BO_3 (JCPDS card # 23-1034) was also detected. When HCOOH and CH_3COOH react with NaBH_4 , they form the sodium salt of anions in a manner similar to that noted with mineral acids. A peak at $2\theta = 32.32^\circ$ corresponding to HCOONa (JCPDS card # 11-0724) and CH_3COONa at $2\theta = 29.98^\circ$ (JCPDS card # 28-1029) are identified along with boron compounds (Fig. 7d and e). In the case of acetic acid, the formation of a hydrated product ($\text{CH}_3\text{COONa}\cdot 3\text{H}_2\text{O}$) is possible as reported in related literature. However, the formation of $\text{CH}_3\text{COONa}\cdot 3\text{H}_2\text{O}$ (JCPDS card # 29-1160 at $2\theta = 29.73^\circ$) has not been clearly identified since the salt and the hydrated species have the same 2θ value. The formation of hydrated products can also be correlated to the lowering of hydrogen yield [33].

Thus, the XRD analysis of the reaction interface indicates that, a host of byproducts can be simultaneously formed as a result of the reaction between NaBH_4 and various types of acidified water. Based on this XRD analysis the specific reactions that occur in the presence of different acids are listed in Table 3. It is noteworthy to mention that the stoichiometric amount of hydrogen generated per mole of the borohydride remains the same irrespective of the type of acid used as accelerator. This allows one to choose either mineral acid or a benign acid to produce hydrogen depending upon the needs of the application. Further it can be noted that CH_3COONa and HCOONa are the byproducts of the reaction with the benign acids. The solubility of these byproducts is very high (97 g per 100 ml of water for HCOONa and 76 g per 100 ml of water for CH_3COONa) [34]. The high solubility of the byproduct means that water associated with the byproducts can reach unreacted NaBH_4 in spite of the absence of any pores (as noted from SEM images) allowing for continued hydrogen generation. This is the reason for higher hydrogen yield with benign acids compared to the HNO_3 and H_3PO_4 .

3.4.3. Effects of borate species on porous pathway formation

A third possibility arises as a result of the unique chemistry of the borate byproducts. From the XRD analysis, it is understood that several reactions lead to the formation of a number of borate compounds (NaBO_2 , B_2O_3 , H_3BO_3 , and $\text{B}(\text{OH})_3$). These borate compounds can be formed with a varying number of water molecules associated with it a few examples of such compounds include borax pentahydrate ($\text{NaB}_4\text{O}_7\cdot 5\text{H}_2\text{O}$) and sodium metaborate dihydrate ($\text{NaBO}_2\cdot 2\text{H}_2\text{O}$) [33,35]. Borates such as $\text{Na}_2\text{B}_4\text{O}_7\cdot 10\text{H}_2\text{O}$, $\text{Na}_2\text{B}_4\text{O}_7\cdot 5\text{H}_2\text{O}$ and H_3BO_3 with $\text{B}:\text{H}_2\text{O}$ ratios of 2:5, 4:5, and 1:0, respectively, are formed by the reaction of acids with solid sodium borohydride. These compounds sequester less water on a per boron atom basis than the borate compounds typically produced by hydrolysis of a sodium borohydride solution, and thus reduce the demand for additional water. Though these hydrated species are difficult to identify through XRD, some literature reports

suggests the possibility of hydrated species formation can be identified through NMR [36]. These hydrated species also facilitates the movement of hydrogen by forming porous structure through diffusion as noted from the SEM images in Fig. 5. In our reactions we have used stoichiometric amount of water and acidified water to enhance hydrogen conversion efficiency. On the other hand, when excess water is used in these reactions, the formation of these hydrated species is predominant. Flooding of the hydrated borates will stabilize the reaction medium and decrease the reaction rate and consequently the hydrogen yield.

These observations confirm that several factors, proposed earlier, contribute to the hydrogen generation rates and yield in heterogeneous small scale systems. Instantaneous generation of large volumes of hydrogen and byproduct solubility can manipulate the porosity, roughness, and liquid transport. Such interfacial transformation influences the free movement of liquid to the unreacted borohydride and alters the hydrogen yield. The proposed system is unique in that a simple one-step catalyst-free hydrogen generation from borohydrides by manipulating the pH of the hydrolysis media is presented. At extremely small dimensions we believe that this system can be user friendly as it can help mitigate the issues that can be a limitation with catalyst based systems.

4. Conclusions

The effects of the addition of several mineral and benign acids on the catalyst-free efficient production of hydrogen from solid borohydride using a small scale device have been demonstrated. A diffusion type contact provides higher hydrogen yield with 70% of the hydrogen delivered in half the time compared to a flow through type device. Acid concentration and surface morphology change are identified as critical to the production of hydrogen with high yield in the absence of catalyst. Three chemical systems were found most promising to produce hydrogen with very high efficiencies (~90%). These include, 97% of hydrogen yield (NaBH_4 and 3N HCl), 96% (NaBH_4 and 3N H_2SO_4), and 87% (NaBH_4 and 12N HCOOH). The hydrogen generation rates, salt composition, and borate formation are likely to influence the interface morphology and are critical to maintain continued contact between the reactants to maximize hydrogen yield.

Acknowledgements

The authors would like to thank the department of defense, advanced projects research agency (DARPA) for the funds provided for this project. Contributions from Dr. Likun Zhu for reactor fabrication are also acknowledged. Useful discussions with Professors Mark Shannon and Richard Masel of University of Illinois are greatly appreciated.

Appendix A. Supplementary data

Supplementary data associated with this article can be found, in the online version, at doi:10.1016/j.jpowsour.2008.10.060.

References

- [1] R.K. Ahluwalia, X.H. Wang, J. Power Sources 177 (2008) 167–176.
- [2] P.P. Prosin, P. Gislou, J. Power Sources 161 (2006) 290–293.
- [3] J.L. Pearce, B. Powers, C. Hess, P.E. Rybski, S.A. Stoeter, N. Papanikolopoulos, J. Intell. Rob. Syst. 45 (2006) 307–321.
- [4] A. Kundu, J.H. Jang, J.H. Gil, C.R. Jung, H.R. Lee, S.H. Kim, B. Ku, Y.S. Oh, J. Power Sources 170 (2007) 67–78.
- [5] X.G. Zhang, D. Zheng, T. Wang, C. Chen, J.Y. Cao, J. Yan, W.M. Wang, J.Y. Liu, H.H. Liu, J. Tian, X.X. Li, H. Yang, B.J. Xia, J. Power Sources 166 (2007) 441–444.
- [6] B. Emonts, J.B. Hansen, H. Schmidt, T. Grube, B. Hohlein, R. Peters, A. Tschauder, J. Power Sources 86 (2000) 228–236.

Table 3

The different reactions that occur during hydrolysis of NaBH_4 with mineral and benign acids.

Reaction	Mineral acids
1.	HCl: $\text{NaBH}_4 + \text{HCl} + 3\text{H}_2\text{O} \rightarrow \text{NaCl} + \text{H}_3\text{BO}_3 + 4\text{H}_2$
2.	H_2SO_4 : $2\text{NaBH}_4 + \text{H}_2\text{SO}_4 + 6\text{H}_2\text{O} \rightarrow \text{Na}_2\text{SO}_4 + 2\text{H}_3\text{BO}_3 + 8\text{H}_2$
3.	H_2SO_4 : $2\text{NaBH}_4 + \text{H}_2\text{SO}_4 + 6\text{H}_2\text{O} \rightarrow \text{Na}_2\text{SO}_4 + 2\text{B}(\text{OH})_3 + 8\text{H}_2$
4.	H_2SO_4 : $2\text{NaBH}_4 + \text{H}_2\text{SO}_4 + 6\text{H}_2\text{O} \rightarrow \text{Na}_2\text{SO}_4\cdot 3\text{H}_2\text{O} + \text{B}_2\text{O}_3 + 8\text{H}_2$
5.	HNO_3 : $\text{NaBH}_4 + \text{HNO}_3 + 3\text{H}_2\text{O} \rightarrow \text{NaNO}_3 + \text{H}_3\text{BO}_3 + 4\text{H}_2$
6.	H_3PO_4 : $3\text{NaBH}_4 + \text{H}_3\text{PO}_4 + 9\text{H}_2\text{O} \rightarrow \text{Na}_3\text{PO}_4 + 3\text{H}_3\text{BO}_3 + 12\text{H}_2$
Reaction	Benign acids
7.	HCOOH : $\text{NaBH}_4 + \text{HCOOH} + 3\text{H}_2\text{O} \rightarrow \text{HCOONa} + \text{H}_3\text{BO}_3 + 4\text{H}_2$
8.	CH_3COOH : $\text{NaBH}_4 + \text{CH}_3\text{COOH} + 3\text{H}_2\text{O} \rightarrow \text{CH}_3\text{COONa} + \text{H}_3\text{BO}_3 + 4\text{H}_2$
9.	CH_3COOH : $\text{NaBH}_4 + \text{CH}_3\text{COOH} + 5\text{H}_2\text{O} \rightarrow \text{CH}_3\text{COONa}\cdot 2\text{H}_2\text{O} + \text{H}_3\text{BO}_3 + 4\text{H}_2$

- [7] J. Pukrushpan, A. Stefanopoulou, S. Varigonda, J. Eborn, C. Haugstetter, *Control Eng. Pract.* 14 (2006) 277–293.
- [8] S.I. Orimo, Y. Nakamori, J.R. Eliseo, A. Zuttel, C.M. Jensen, *Chem. Rev.* 107 (2007) 4111–4132.
- [9] R. Aiello, M.A. Matthews, D.L. Reger, J.E. Collins, *Int. J. Hydrogen Energy* 23 (1998) 1103–1108.
- [10] J.H. Wee, K.Y. Lee, S.H. Kim, *Fuel Process. Technol.* 87 (2006) 811–819.
- [11] Z.T. Xia, S.H. Chan, *J. Power Sources* 152 (2005) 46–49.
- [12] S.C. Amendola, S.L. Sharp-Goldman, M.S. Janjua, M.T. Kelly, P.J. Petillo, M. Binder, *J. Power Sources* 85 (2000) 186–189.
- [13] S.C. Amendola, S.L. Sharp-Goldman, M.S. Janjua, N.C. Spencer, M.T. Kelly, P.J. Petillo, M. Binder, *Int. J. Hydrogen Energy* 25 (2000) 969–975.
- [14] D.Y. Xu, H.M. Zhang, W. Ye, *Prog. Chem.* 19 (2007) 1598–1605.
- [15] C.L. Hsueh, C.Y. Chen, J.R. Ku, S.F. Tsai, Y.Y. Hsu, F.H. Tsau, M.S. Jeng, *J. Power Sources* 177 (2008) 485–492.
- [16] S.U. Jeong, E.A. Cho, S.W. Nam, I.H. Oh, U.H. Jung, S.H. Kim, *Int. J. Hydrogen Energy* 32 (2007) 1749–1754.
- [17] Y. Chen, H. Kim, *Mater. Lett.* 62 (2008) 1451–1454.
- [18] H. Dong, H.X. Yang, X.P. Ai, C.S. Cha, *Int. J. Hydrogen Energy* 28 (2003) 1095–1100.
- [19] C. Wu, Y. Bai, F. Wu, G.Q. Wang, *Trans. Nonferrous Met. Soc.* 17 (2007) S1002–S1005.
- [20] S.C. Amendola, M. Binder, S.L. Sharp-Goldman, M.T. Kelly, P.J. Petillo, *US* 6,534,033 B1 (2003).
- [21] S.C. Amendola, M. Binder, S.L. Sharp-Goldman, M.T. Kelly, P.J. Petillo, *US* 6,683,025 B2 (2004).
- [22] S.C. Amendola, P.J. Petillo, S.C. Petillo, R.M. Mohring, *US* 6,932,847 B2 (2005).
- [23] J.S. Wainright, R.F. Savinell, C.C. Liu, M. Litt, *Electrochim. Acta* 48 (2003) 2869–2877.
- [24] P.B. Koeneman, I.J. BuschVishniac, K.L. Wood, *J. Microelectromech. Syst.* 6 (1997) 355–362.
- [25] O.J. Kwon, S.M. Hwang, J.G. Ahn, J.J. Kim, *J. Power Sources* 156 (2006) 253–259.
- [26] L.L. Zhang, T.H. Lu, J.C. Bao, Y.W. Tang, C. Li, *Electrochem. Commun.* 8 (2006) 1625–1627.
- [27] Y. Shang, R. Chen, *Energy Fuels* 20 (2006) 2142–2148.
- [28] R.E. Davis, E. Bromels, C. Kibby, *J. Am. Chem. Soc.* 84 (1962) 885–892.
- [29] H.I. Schlesinger, H.C. Brown, A.E. Finholt, J.R. Gilbreath, H.R. Hoekstra, E.K. Hyde, *J. Am. Chem. Soc.* 75 (1952) 215–216.
- [30] D.H. Ripin, D.A. Evans, *pK_a's of inorganic and oxo-acids*, <http://www2.lsddiv.harvard.edu/labs/evans/index.html>, Harvard, 2005.
- [31] I.M. Kolthoff, in: I.M. Kolthoff (Ed.), *Treatise of Analytical Chemistry*, First ed., Interscience Publishers, New York, 1959.
- [32] V. Maemets, I. Koppel, *J. Chem. Soc., Faraday Trans.* 92 (1996) 3533–3538.
- [33] E.Y. Marrero-Alfonso, J.R. Gray, T.A. Davis, M.A. Matthews, *Int. J. Hydrogen Energy* 32 (2007) 4723–4730.
- [34] S.L. Phillips, L.D. Perry (Eds.), *Handbook of Inorganic Compounds*, First ed., CRC press, Florida, 1995, p. 528.
- [35] N.P. Nies, R.W. Hulbert, *J. Chem. Eng. Data* 12 (1967) 303–313.
- [36] Q. Zhang, R.M. Mohring, Y. Wu, *EP20050733671* (2007).